Ly. J. Appl. Sci. Tech. V. 14, No (1). 43-50
Libya Journal of Applied Sciences and Technology
https://ljast.ly/

Finite Element Analysis of Thermal and Residual Stress Fields in TIG-Welded Copper-to-Brass Dissimilar Joints

Hamza I. M Shormit, Khaled I. Azzabi*, and Mohamed Tuhami Swei

Department of Mechanical and Industrial Engineering, College of Engineering Technology Janzour, Tripoli, Libya.

Khaled I. Azzabi*: azzabikh@cetj.edu.ly

Article Info

Received: 01/06/2026
Accepted: 12/06/2026
Online publish: 23/06/2026

Keywords:
Dissimilar welding;
Transient thermal analysis;
Stress distribution;
Finite element analysis;

Abstract

This study investigates a finite element analysis (FEA) of a dissimilar welded assembly consisting of a pure copper tube (C11000) and a brass flange, joined via the tungsten inert gas (TIG) welding process using ERCuSn-A filler metal. Numerical simulations were conducted using SolidWorks Simulation to evaluate the thermo-mechanical response of the joint under specific operating conditions. The research encompasses a transient thermal analysis of the welding process, followed by a static assessment of stress distribution and deformations induced by combined thermal and mechanical loading. The findings underscore the inherent challenges of joining dissimilar materials and demonstrate the critical influence of joint geometry on the assembly's structural integrity.

التحليل بالعناصر المحدودة لحقول الإجهاد الحراري والمتبقي في الوصلات غير المتماثلة للحام النحاس بالأرجون (TIG) بين النحاس الأحمر والنحاس الأصفر

حمزة إسماعيل شرميط *، خالد إبراهيم العزابي ، محمد التوهامي

قسم الهندسة الميكانيكية والصناعية، كلية التقنية الهندسية جنزور، طرابلس، ليبيا

تتناول هذا المقالة دراسة بطريقة تحليل العناصر المحدودة (*FEA*) لقطعة معدنية تتكون من أنبوب نحاسي وفلانجة (*Flange*) من النحاس الأصفر (*Brass*) وباستخدام سلك لحام *ERCuSn-A*، يتم لحامهما باستخدام تقنية لحام التيغ (*TIG*). أُجريت المحاكاة باستخدام أدوات *SolidWorks Simulation* بهدف تحليل السلوكين الحراري والستاتيكي تحت ظروف تشغيل محددة. تشمل الدراسة تحليل انتقال الحرارة الناتج عن اللحام، يليه تحليل ستاتيكي لتوزيع الإجهادات والتشوهات الناتجة عن التأثيرات الحرارية والميكانيكية. تُبرز النتائج التحديات المرتبطة بلحام مواد غير متجانسة وتأثير الشكل الهندسي على الأداء البنيوي للوصلة.

الكلمات المفتاحية

لحام المواد غير المتشابهة، التحليل الحراري العابر، توزيع الإجهادات، تحليل العناصر المحدودة

1. Introduction

This study investigates a TIG-welded joint between a brass flange and a copper tube, utilizing ERCuSn-A filler metal [2,5]. The joint configuration is representative of geometries commonly found in fluid handling systems. Brass was selected for the flange component due to its superior mechanical properties compared to pure copper, as detailed in Table 1 [4]. The enhanced mechanical stability of brass justifies this selection [1,3]; the comparative data underscore the rationale for this material choice. Furthermore, brass flanges are integral to hot water, refrigeration, and gas distribution systems, where sealing gaskets are typically employed between the flange face and mating components.

Table 1. Comparative Mechanical and Practical Properties of Brass and Copper

Aspect	Brass	Copper	Added Value of Brass
Hardness	Higher (70–90 HB)	Lower (40–50 HB)	Withstands torque and bolt clamping pressure
Machinability	Excellent (90–100%)	Poor (~20%)	Easier to turn, drill, and machine precision holes
Deformation resistance under load	Superior due to crystalline structure	Poor; deforms readily	Maintains flange alignment during fastening
Dimensional stability during machining	Excellent	Moderate	Yields smoother, more accurate mating surfaces
Friction and wear resistance at mechanical contact	High (abrasion-resistant)	Relatively low	Ideal for contact surfaces with gaskets and bolts
Cost	Less expensive than pure copper	Significantly more expensive	Overall cost savings

2. Methodology

2.1 Geometric Model

The three-dimensional (3D) CAD model of the welded assembly was developed using SolidWorks. The assembly comprises a cylindrical copper tube (Outer Diameter [OD] 30 mm, wall thickness 4 mm) joined to a flat brass flange (OD 63 mm, height 7 mm), as illustrated in Figure 1. The geometry was precisely modeled to ensure high-fidelity representation during the subsequent finite element discretization.

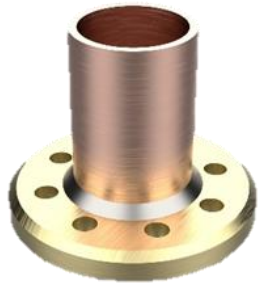

Figure 1. Three-dimensional geometric model of the copper tube–brass flange welded assembly (SolidWorks)

2.2 Welding Parameters and Process Data

The welding process parameters were defined before the simulation to calculate the net heat input, which was subsequently implemented as a transient thermal load in the finite element model. Table 2 summarizes the optimized TIG welding specifications adopted for this investigation [2,5], ensuring that the simulated thermal cycles align with realistic welding conditions.

Table 2. TIG Welding Machine Settings

Parameter	Recommended Setting
Current type	DC (straight polarity/electrode negative)
Arc voltage	15 V
Welding current	160 A
Shielding gas	Argon + Helium (75% Ar + 25% He) for enhanced heat penetration
Gas flow rate	12–15 L/min
Tungsten electrode diameter	3.2 mm (ground to a 15–30° included angle)
Filler wire (ERCuSn-A)	Diameter: 2.4 mm
Torch angle	10–15° from the vertical (to concentrate heat on the thicker flange)
Welding speed	6 cm/min (to control heat input)

2.3 Weld Time and Heat Power Calculations

The weld seam length was determined from the tube circumference:

$$L = \pi \times d = 3.14 \times 30 \approx 94.2\ mm.$$

At a welding speed of 6 cm/min (60 mm/min), the arc travel time is:

$$t = 94.2\ mm \div 60\ mm/min \approx 94\ s.$$

Allowing an additional 8 seconds for the cooling initiation phase yields a total simulation duration of **102** seconds. The effective heat input was calculated from the welding parameters recorded in Table 2. With an arc voltage of **15 V**, a welding current of **160 A**, and an assumed thermal efficiency of **η = 0.70** (consistent with the 60–80% range characteristic of TIG welding, in which a fraction of the generated energy is lost to the shielding gas and surroundings):

$$\boldsymbol{P = V \times I \times \eta = 15\ V \times 160\ A \times 0.70 \approx 1{,}680\ W}$$

For the simulation, a rounded value of **1,650 W** was applied as the prescribed heat power per weld segment.

2.4 Assumptions and Model Simplifications

To facilitate the computational analysis within the current software framework, several simplifying assumptions were implemented:

- Linear Material Behavior: The analysis assumes linear elastic behavior for both base metals and the filler rod.
- Constant Material Properties: Thermal and mechanical properties (e.g., thermal conductivity, specific heat, and yield strength) are treated as temperature-independent constants.
- Phase Change Neglect: The latent heat of fusion and vaporization was not explicitly modeled, focusing instead on the macro-thermal distribution.

- Stepwise Heat Application: The moving heat source was approximated by sequential heat load application across discrete segments of the weld path.

These simplifications define the study as a first-order approximation intended to identify qualitative trends rather than absolute quantitative values.

3. Discussion

3.1 Steady-State Thermal Analysis

The simulation sequence commenced with a steady-state thermal analysis to establish a spatially uniform temperature distribution throughout the assembly. This baseline serves as the prescribed initial condition for the subsequent transient thermal analysis, which characterizes the dynamic welding cycle. To ensure numerical accuracy, material properties were defined for each component by developing customized profiles within the SolidWorks material database. The thermo-physical properties utilized for pure copper (C11000) are summarized in Table 3 [4].

Table 3. Material Properties: Pure Copper (C11000)

Property	Value	Units
Elastic Modulus	110,000	N/mm^2
Poisson's Ratio	0.34	—
Shear Modulus	46,000	N/mm^2
Mass Density	8,940	kg/m^3
Yield Strength	70	N/mm^2
Thermal Expansion Coefficient	1.7×10^{-5}	/K
Thermal Conductivity	385	W/(m·K)
Specific Heat	385	J/(kg·K)

The corresponding properties of the filler metal, ERCuSn-A, are presented in **Table 4 [4]**.

Table 4. Material Properties: Filler Metal ERCuSn-A

Property	Value	Units
Elastic Modulus	110,000	N/mm^2
Poisson's Ratio	0.341	—
Shear Modulus	44,000	N/mm^2
Mass Density	8,800	kg/m^3
Yield Strength	455	N/mm^2
Thermal Expansion Coefficient	1.84×10^{-5}	/K
Thermal Conductivity	100	W/(m·K)
Specific Heat	380	J/(kg·K)

The material properties assigned to the brass (Brass) flange are given in Table 5 [4].

Table 5. Material Properties: Brass

Property	Value	Units
Elastic Modulus	100,000	N/mm^2
Poisson's Ratio	0.33	—
Shear Modulus	37,000	N/mm^2
Mass Density	8,500	kg/m^3
Yield Strength	240	N/mm^2
Thermal Expansion Coefficient	1.8×10^{-5}	/K
Thermal Conductivity	110	W/(m·K)
Specific Heat	390	J/(kg·K)

Following the material property assignment, an initial temperature of 300 K was prescribed to the entire assembly, representing a thermal equilibrium state with the ambient environment. In this study, natural convection was assumed without forced airflow. Subsequently, the finite element mesh was generated, and the numerical solver was executed to obtain the steady-state thermal distribution.

3.2 Transient Thermal Analysis

Since SolidWorks Simulation does not natively support a moving heat source, a discrete approximation strategy was implemented to simulate the welding process. The circular weld seam was discretized into 16 arc segments of equal length. A time-dependent thermal load was sequentially applied to each segment, with a torch dwell time of 6 seconds per segment — a duration calculated to account for the substantial thermal mass of the brass flange. This segmented application approximates the transient progression of the weld pool along the joint circumference, effectively capturing the thermal oscillation patterns as illustrated in Figure 2.

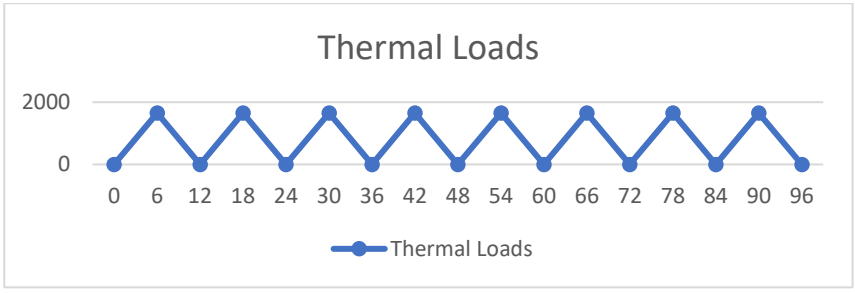

Figure 2. Time–heat-load schedule: temporal activation and deactivation of the 16 weld-segment heat sources over the 96-second arc-on period

The analysis was transitioned to a Transient Thermal Study, with a total simulation duration of 102 seconds and a fixed time-step increment of 1 second. To ensure continuity, the temperature profile obtained from the steady-state analysis was imported as the prescribed initial condition for this stage. This temporal discretization was selected to adequately capture the rapid thermal cycles associated with the TIG welding process.

A prescribed heat power of 1,650 W was assigned to each of the 16 segments via the Use Time Curve option.

Convective heat loss from all external surfaces exposed to the environment was accounted for by prescribing a surface convection boundary condition. A convection coefficient (h) of 25 $W/(m^2 \cdot K)$

was utilized, representing the upper bound of the standard range (10–25 W/(m^2·K)) typical for natural convection in stagnant air. The ambient (sink) temperature was maintained at 300 K, ensuring consistency with the previously established initial conditions. The comprehensive thermal loading sequence, encompassing all 16 discrete heat-power applications is presented.

Upon completion of the mesh generation and numerical computation, the transient temperature field was resolved, as illustrated in Figure 3. A plan-view projection depicts the spatial temperature distribution at the conclusion of the heating cycle.

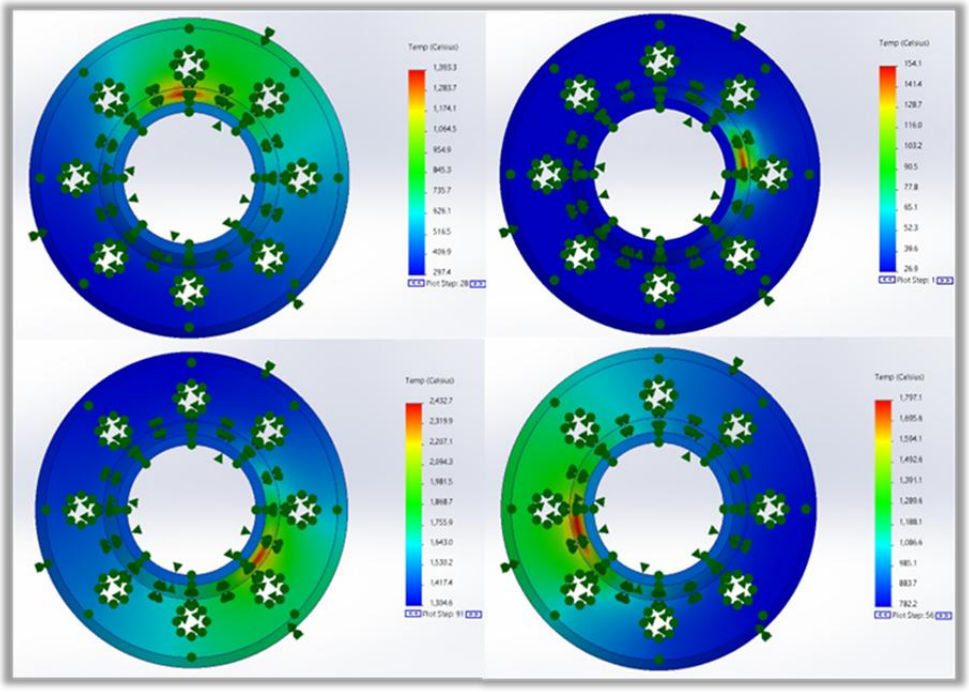

Figure 3. Plan-view temperature distribution from Transient Thermal Analysis — full-field result at end of heating phase

The peak temperature recorded within the arc plasma zone has reached 2,556 °C.

It is noteworthy that the vaporization temperature of copper is approximately 2,560 °C, indicating that the simulated peak temperature approaches the physical evaporation threshold of the base metal.

3.3 Static Structural Analysis

A linear static structural analysis was performed to quantify the thermally induced stresses and deformations accumulated in the assembly. The study was initialized by importing the material definitions from previous studies. The transient temperature field was then coupled to the structural solver as an imported thermal load.

Upon mesh generation and solution, the resultant displacement field was post-processed. The total displacement contour representing the thermally induced deformation of the assembly is presented in Figure 4.

The maximum displacement was found to be 0.031 mm. This magnitude is negligibly small for most engineering applications that do not impose sub-millimeter geometric tolerances. It should be noted that SolidWorks Simulation intentionally renders the deformed shape at an amplified scale for visualization purposes; the displacement magnitudes shown in the contour plot do not represent actual dimensional changes.

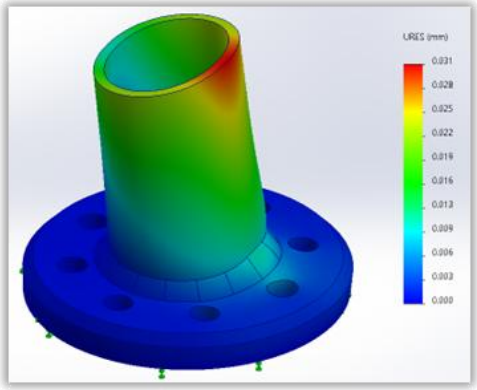

Figure 4. Total displacement contour from the static structural analysis (thermally induced deformation)

4. Results

4.1 Thermal Analysis Results

The thermal analysis results reveal an elevated and highly localized heat flux within the weld zone during the heating phase, driven by the sequential application of the arc heat source across the sixteen weld segments. The following observations were made:

- The maximum temperature within the weld region reached approximately 2,556 °C, a value that approaches the vaporization temperature of copper.
- Following cessation of the heat input, the cooling-phase results demonstrate that the assembly returned progressively and smoothly to ambient temperature.

4.2 Static Structural Analysis Results

The spatially resolved temperature field from Transient Thermal Analysis served as the thermal loading input for the structural analysis. The simulation captured the elastic response of the assembly to differential thermal expansion and contraction during and after the welding cycle. The principal findings are as follows:

- Residual thermal stresses were concentrated at and immediately adjacent to the weld interface; the maximum von Mises equivalent stress reached approximately 183.9 MPa.
- A maximum total displacement of 0.031 mm was recorded, localized predominantly within the weld zone. This level of deformation is well within acceptable limits for most engineering service conditions.

5. Conclusions and Recommendations

It must be acknowledged that SolidWorks Simulation possesses inherent limitations that constrain the high-fidelity modeling of welding processes. Specifically, the software does not natively support a spatially distributed moving heat source—such as the Gaussian or Goldak double-ellipsoid formulations -nor does it incorporate 'element birth-and-death' algorithms required to simulate the progressive deposition of filler metal. The absence of these advanced constitutive models limits the physical accuracy of the simulation [6,7]; consequently, the present results should be interpreted as a first-order approximation rather than a definitive representation of the joint's complex thermo-mechanical behavior.

To overcome these constraints and achieve a more rigorous characterization of the Heat-Affected Zone (HAZ), microstructural evolution, and complex residual stress states, it is recommended that future research utilize specialized welding simulation frameworks, such as ANSYS or Simufact Welding, which offer purpose-built tools for advanced joining analysis [7].

In conclusion, this research provides a baseline understanding of the joining process for copper and brass. Future studies should transition toward non-linear, temperature-dependent models and incorporate experimental validation to refine the precision of the predicted residual stress states.

Conflict of Interest

The Author(s) declares that there is no conflict of interest.

Authors' Contributions

Hamza I. M Shormit contributed to simulation setup, thermo-mechanical result analysis. Khaled I. Azzabi, contributed to simulation validation, verification of finite element modeling procedures.

Mohamed Tuhami Swei, contributed interpretation of welding-induced stress and temperature fields, manuscript reviewing and editing, technical presentation enhancement, and reference verification.

Fundings

This research received no specific grant.

Data Availability

Data are available from the corresponding author upon reasonable request.

6. References

[1]. Jha, Sujit, Balakumar, Devibala, Paluchamy, & Rajalingam. (2015). Experimental analysis of microstructure and mechanical properties of copper and brass-based alloys, https://doi.org/10.15282/ijame.11.2015.14.0195.

[2]. American Welding Society (AWS). (2020). AWS A5.7: Specification for Bare Rods and Electrodes for Gas Shielded Arc Welding of Copper and Copper Alloys.

[3]. Davis, J. R (2001). Alloying: Understanding the basics. ASM International

[4]. ASM International. (1990). Properties and Selection: Nonferrous Alloys and Special-Purpose Materials. *ASM Handbook, Vol. 2.*

[5]. ASM Handbook. (1993) Welding, Brazing, and Soldering, Vol. 6.

[6]. Goldak, J., Chakravarti, A., & Bibby, M. (1984). A new finite element model for welding heat sources. Metallurgical Transactions B, 15, 299–305. https://doi.org/10.1007/BF02667333

[7]. Vemanaboina, H., Akella, S., & Buddu, R. K. (2014). Welding process simulation model for temperature and residual stress analysis. Procedia Materials Science, 6, 1539–1546. https://doi.org/10.1016/j.mspro.2014.07.135